Cement and Concrete Composites 88 (2018) 130–138

Contents lists available at ScienceDirect

Cement and Concrete Composites

journal homepage: www.elsevier.com/locate/cemconcomp

Mineral wool production waste as an additive for Portland cement

Raimonda Kubiliute, Rimvydas Kaminskas*, Akvile Kazlauskaite

Department of Silicate Technology, Faculty of Chemical Technology, Kaunas University of Technology, Radvilenu str. 19, LT-50254, Kaunas, Lithuania

ARTICLE INFO

Article history:
Received 8 September 2017
Received in revised form
23 November 2017
Accepted 5 February 2018
Available online 8 February 2018

Keywords:
Mineral wool cupola dust
Chloride
Portland cement
Hydration
Compressive strength

ABSTRACT

This study aims at investigating the possibility of using dust, collected in air filters during the melting of mineral wool raw materials (mineral wool cupola dust) as an additive for Portland cement. It was found that the investigated dust mainly consists of quartz, periclase, albite, dolomite, and the amorphous phase. The main impurities are halite and sylvite. The investigated additive was additionally milled and prepared as a microfiller. The results showed that the cupola dust additive increases the initial hydration of cement, yet prolongs the dormant period. It was estimated that up to 15 wt% of Portland cement can be replaced by the dust additive without impairing the strength properties of samples after 28 days of hardening. However, after 90 days of hydration, the compressive strength of all samples with the investigated additive is lower than in pure OPC samples. This phenomenon is concerned with the formation of a significant amount of Friedel's salt. The content of chlorides in the raw material was reduced from 4.901 to 0.612 wt% by washing with water, when the water-to-solid ratio was equal to 10. The results of the investigation showed that the washed and ground cupola dust had a positive effect on the compressive strength of the cement samples. When 5, 10, and 15 wt% of prepared dust additive were used, the compressive strength of samples after 28 and 90 days of hydration was greater than that of pure Portland cement sample. The findings suggest that the additionally prepared dust additive leads to the formation of a stable structure of the cement stone, accelerates the calcium silicates hydration, and promotes the formation of gismondine.

1. Introduction

One of the major priorities in cement industry is to find materials that may be used as a clinker replacement and which could help in reducing energy consumption and CO_2 emissions during cement production [1]. Special attention is paid to the replacement of a part of ordinary Portland cement with various industrial mineral wastes [2,3]. The fine additives used in cement systems are classified into reactive and inert substances [4]. Reactive additives can chemically react with Portland cement hydrates (as a pozzolanic reaction), while inert additives in normal processing conditions fill up the void spaces remaining between the coarser particles and contribute to the increase of the compressive strength without any chemical reaction [4,5]. The addition of pozzolans to Portland cement increases its mechanical strength and durability compared with the blank paste because of the interface reinforcement [6], whereas the microfiller effect depends mainly on the shape and size of the particles, particle size distribution, and specific surface area [7].

Research of economic binders through the use of industrial by-products (blast furnace slag, silica fume, fly-ashes, rice husk ashes, and other materials) is a major concern in reducing the deficit recorded during the manufacture of Portland cement [8]. A new source of an additive for Portland cement could be found in a waste product from mineral wool industries. The term “mineral wool” is a general name for fibre materials that are formed by spinning or drawing molten minerals. The chemical composition of these minerals mainly consists of SiO_2, Al_2O_3, CaO, and MgO, whereas other oxides are considered as impurities [9].

During the mineral wool production process, the waste materials such as fibre waste and cupola dust form. On the one hand, mineral wool fibre waste can be recycled and returned to the production line, but cupola dust is usually sent to the waste dump. On the other hand, rock wool fibre waste can be used as a suitable substitute for coarse and fine aggregates, saving on the cost of natural aggregates and minimising the environmental impact of solid waste disposal [10]. Some researchers [10] also note that the composition of rock wool fibre waste is similar to other pozzolana

* Corresponding author.
E-mail address: rimvydas.kaminskas@ktu.lt (R. Kaminskas).

https://doi.org/10.1016/j.cemconcomp.2018.02.003
0958-9465/

materials such as fly ash, ground granulated blast-furnace slag (GGBS), and silica fume. The reactive additives cause a compaction of the matrix and interface transition zone because the particles of pozzolanic materials fill the void space between the larger grains, which is otherwise occupied by water, and, with time, they react chemically to produce additional hydrates [11,12].

It has been found that rock wool wastes can act as either a cementitious material or an inert filler in cement-based composites, depending on the particle size. The dense structure of cement-based composite, achieved by the filling effect of pozzolanic product, improves the compressive strength, splitting tensile strength, abrasion resistance, absorption, resistance to potential alkali reactivity, and resistivity [5,10]. In addition, it was pointed out [13] that 10–40 wt% of mineral wool fibre waste additive reduced porosity and changed the microstructure of the cement-based composites. These effects impair chloride ion and other ion penetration/mobility.

However, there has been little discussion on the use of other mineral wool production process wastes such as cupola dust. This waste is accumulated in the filters for air coming out of the cupola and comprised of raw materials, additives, and melted particles mixture. Thus, cupola dust is very dispersive, with strong sorption properties [14,15].

It was reported [16] that the cupola dust additive, through its grading and chemical composition, reduces significantly the cement paste spreadability. Moreover, it was found that this additive had an influence on the hydration process of Portland cement and increased the early strength of hardened cement paste [16]. The aim of this work was to determine the possibility of using dust collected in filters, during the production of mineral wool, as an additive for the Portland cement.

2. Materials and methods

In this work, mineral wool manufacturing waste, cupola dust, was used. Different modifications of this by-product were prepared: ground cupola dust (RWCD) and additionally washed cupola dust (WRWCD). The raw cupola dust was ground with a Fritsch planetary disc mill Pulverisette 9 for 120 s at 600 rpm to a specific surface area of 400 m^2/kg. Cupola dust was washed with water when water-to solid ratio was w/s = 10. After 1, 5, and 10 min stirring of suspension, the residue was filtered off through a Buchner funnel and dried at 70 °C temperature.

The chemical composition of the ground (RWCD) and washed cupola dust (WRWCD) is shown in Table 1.

Ordinary Portland cement CEM I 42.5 R was chosen in this work. The chemical composition of the Portland cement is shown in Table 1. The mineralogical composition of the clinker was as follows: $3CaO \cdot SiO_2$, 52.97 wt%; $2CaO \cdot SiO_2$, 19.61 wt%; $3CaO \cdot Al_2O_3$, 9.16 wt%; $4CaO \cdot Al_2O_3 \cdot Fe_2O_3$, 9.74 wt%; $CaSO_4 \cdot 2H_2O$, 5.37 wt%.

The sieve analysis of raw cupola dust was carried out by using Haver EML Digital Plus sieve shaker combined with ⌀ 5, 2, 1.6, 1, 0.5, 0.315, 0.2, 0.16, 0.08 mm sieves. The mass of the sample was 300 g, time of sieving – 15 min and the amplitude of the oscillation frequency – 1.5.

The particle size distribution and the specific surface area of the materials were determined by a laser particle size analyser (CILAS 1090 LD) in intervals from 0.1 to 500 μm. The distribution of solid particles in the air stream was 12–15 wt%. Compressed air (5000 mbar) was used as a dispersing phase. The measuring time was 15 s.

The amount of Cl^- ions in the investigated materials was determined by a Mohr's method [17].

The pozzolanic activity was assessed using a modified Chapelle method [18]. This test consists of placing 1.000 g of mineral admixture into 500 ml of lime solution (1.200 g/l CaO). The solution was kept for the first 48 h in a thermostat at 45 °C. At the end of this period, 50 ml of the solution was taken and the CaO content was determined by the titration with 0.05 N hydrochloric acid (HCl) solution using methyl orange as an indicator. The results were expressed by milligrams of bounded CaO per gram of a pozzolanic additive. The rest of the solution (450 ml) was kept again for 24 h at 45 °C. The process was repeated until the estimated value of the pozzolanic activity was insignificantly low (7 days).

The hydraulic activity of RWCD also was estimated by a Frattini test (EN 196-5) [19].

The samples (30 × 30 × 30 mm) were formed of pure ordinary Portland cement and Portland cement with 5, 10, 15, and 20% (by weight) replacement with the investigated additive. The samples were stored in molds at 20 ± 1 °C and 100% humidity during the first day of hydration. After 24 h of hydration, the samples were transferred to deionised water and were stored there for 6, 27 and 89 days at 20 ± 1 °C. The hydration of samples was stopped using acetone: three samples were kept under the conditions described; then samples were crushed separately, milled together using a laboratory planetary disc mill, passed through an 80-μm sieve, washed with acetone, and dried in CO_2 free atmosphere at 65 ± 5 °C for 8 h. A representative amount was selected from the lot to be analysed, which, upon further quartering (EN 196-2, EN 196-7 [20,21]), was reduced to a manageable amount for appropriate sample preparation. Powder samples were stored in sealed bags to prevent carbonation and hydration.

The XRD analysis was performed on the D8 Advance diffractometer (Bruker AXS, Karlsruhe, Germany) operating at the tube voltage of 40 kV and tube current of 40 mA. The X-ray beam was filtered with Ni 0.02 mm filter to select the CuKα wavelength. Diffraction patterns were recorded in a Bragg-Brentano geometry using a fast counting detector Bruker LynxEye based on the silicon strip technology. The specimens of samples were scanned over the range $2\theta = 3–70°$ at a scanning speed of 6° min^{-1} using a coupled two theta/theta scan type.

The chemical composition analysis of samples was performed by X-ray fluorescence spectroscopy (XRF) on a Bruker X-ray S8 Tiger WD spectrometer equipped with a Rh tube with energy of up to 60 keV. The measurements of powder samples were carried out in Helium atmosphere and data were analysed with SPECTRA Plus QUANT EXPRESS standard software.

The simultaneous thermal analysis (STA) (differential scanning calorimetry and thermogravimetry) was carried out on a Netzsch STA 409 PC Luxx instrument with ceramic sample handlers and crucibles of Pt-Rh. At a heating rate of 15 °C/min, the temperature ranged from 30 °C to 900 °C under the ambient atmosphere.

Table 1
Chemical composition of raw materials.

Material	SiO_2	Al_2O_3	Fe_2O_3	CaO	MgO	K_2O	Na_2O	SO_3	Cl	Loss on ignition, wt.%
OPC	19.52	5.03	3.05	61.39	3.93	1.06	0.12	2.5	≤0.1	–
RWCD	27.04	6.31	8.03	9.57	5.85	5.45	3.43	5.05	4.95	24.32
WRWCD	30.0	6.59	8.66	10.35	6.43	2.92	1.46	4.98	0.61	25.76

The calorimetric analysis data were obtained using a TAM AIR III calorimeter. The range of measurement was ±600 mW, the sensitivity of the signal was 4 μW, the time constant was <500 s, the temperature of the experiment was 25 ± 0.1 °C, and the water-to-solid ratio was 0.5.

3. Results and discussion

3.1. Characterization of mineral wool cupola dust waste

The particle size of raw cupola dust estimated by the laser diffraction is inaccurate because a considerable portion of the particles is larger than 500 μm. The results of the sieve analysis are shown in Fig. 1. The data of sieve analysis show that raw cupola dust particle diameter varies over very wide limits, and particles larger than 80 μm constitute 87.8 wt % of the total amount.

Since the diameter of mineral wool cupola dust particles was almost unequal, the dust was ground with a Fritsch planetary disc mill Pulverisette 9 for 120 s at 600 rpm (specific surface area $S_a = 400\ m^2/kg$). The particle size distribution results (Fig. 2) showed that after milling ~95 wt% of the total amount of the dust constituted the particles with the diameter smaller than 63 μm. Therefore, the ground cupola dust (RWCD) prepared this way can be used as a microfiller (EN 12620:2002 + A1:2008 [22]).

According to the X-ray diffraction (XRD) analysis data (Fig. 3), quartz (*d*-spacing: 0.425, 0.344, 0.181 nm; JCPDS 77-1060), periclase (*d*-spacing: 0.210, 0.148 nm; JCPDS 45-946), albite (*d*-spacing: 0.403, 0.321, 0.320, 0.317 nm; JCPDS 72-1246), paragonite (*d*-spacing: 0.963, 0.320, 0.302, 0.252 nm; JCPDS 42-0602), iron sulfite (*d*-spacing: 0.636, 0.285, 0.240, 0.212, 0.154 nm; JCPDS 32-0473), and dolomite (*d*-spacing: 0.288, 0.219, 0.201, 0.180, 0.178 nm; JCPDS 36-0426) were found in RWCD. Furthermore, a broad peak in the angle of diffraction from 18° to 29°, typical for the amorphous component, was fixed in the XRD curve. It was determined that cupola dust contains chlorides: sylvite (*d*-spacing: 0.314, 0.222, 0.181 nm; JCPDS 41-1476) and halite (*d*-spacing: 0.326, 0.282, 0.199, 0.163 nm; JCPDS 5-0628).

Despite the fact that XRD analysis data show the presence of an amorphous component in the composition of RWCD, the pozzolanic activity of the investigated dust (estimated by the modified Chapelle method) was very low and reached only 63 mgCaO/g. To ensure the adequacy of the Chapelle method, the Frattini test (EN 196-5) [19] was also performed (Fig. 4). As expected, the cement samples with the RWCD additive do not satisfy the test for pozzolanicity because the data points of all samples with the RWCD additive are plotted above or on the curve of calcium ion saturation concentration. Therefore, the RWCD additive was used as inert microfiller.

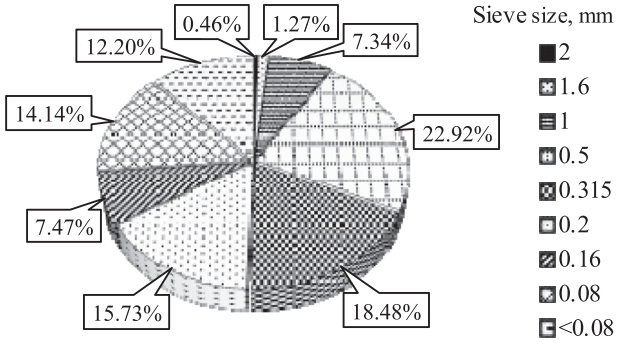

Fig. 1. Sieve analysis results of raw mineral wool cupola dust.

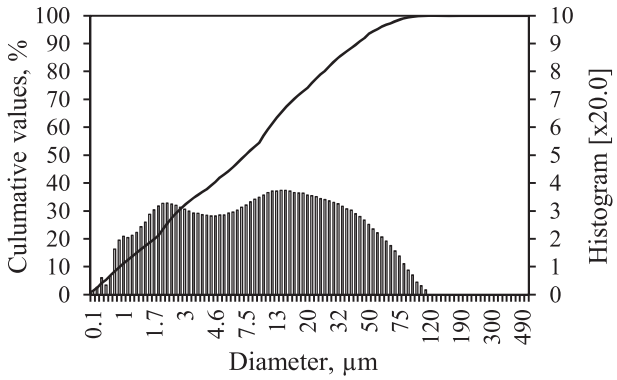

Fig. 2. Particle size distribution of the milled cupola dust.

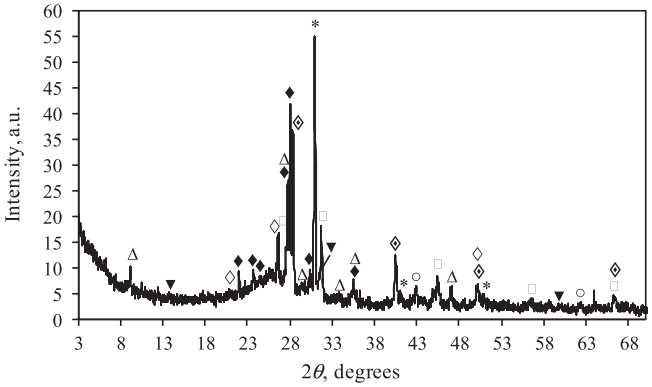

Fig. 3. X-ray diffraction pattern of RWCD. Indexes: * – dolomite ($CaMg(CO_3)_2$); ◊ – quartz (SiO_2); ◆ – albite ($NaAlSiO_3O_8$); ▼ – iron sulfite ($FeSO_3$); ○ – periclase (MgO); □ – halite (NaCl); ⋄ – sylvite (KCl); Δ – paragonite ($NaAl_2(Si_3Al)O_{10}(OH)_2$).

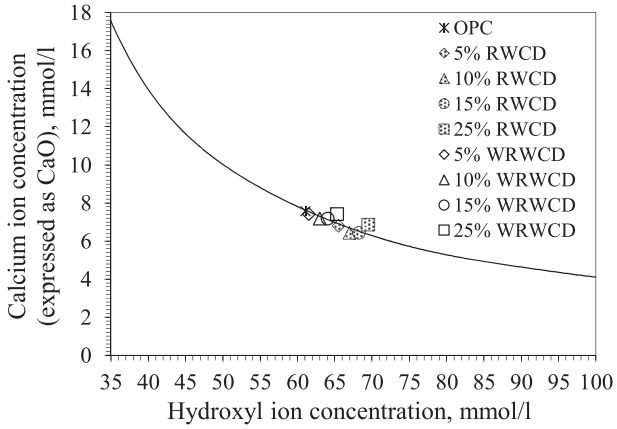

Fig. 4. Results of pozzolanicity tests of investigated mixtures.

3.2. Influence of ground mineral wool cupola dust waste on Portland cement hydration and hardening

Physical tests of the setting time and normal consistency (EN 196-3 [23]) of different cement compositions with the RWCD additive were performed (Table 2). These data show that the RWCD additive has no major influence on the water-to-solid ratio (w/c) for normal consistency of cement pastes. However, it considerably shortened the setting time: the paste began to bind after 80, 60, and 52 min, when, respectively 5, 15, and 20 wt% of the RWCD additive

Table 2
Influence of cupola dust additives on normal consistency and setting time of samples.

Amount of additive, wt.%	Normal consistency (w/c), %		Initial setting time, min		Final setting time, min	
	RWCD	WRWCD	RWCD	WRWCD	RWCD	WRWCD
0	0.255		105		150	
5	0.256	0.256	80	90	142	133
15	0.256	0.261	60	68	102	100
20	0.257	0.263	52	60	82	85

was added. The cement paste also ended to bind through a shorter time. Apparently, a shortened setting time is associated with significant amount of chloride compounds in the composition of the RWCD additive.

It is important to note that 20 wt% is the largest possible amount of RWCD which can be added to the cement, as in accordance with the EN 206:2013 + A1:2016 [24] standard, a maximum chloride ion content by mass of cement should not exceed one percent for chloride class Cl 1.0 concrete.

In the next stage of the research, the measurements on the heat evolution during the hydration process (calorimetric analysis) of cement samples with 5, 15, and 20 wt% RWCD additive were performed (Fig. 5). As shown in Fig. 5 (a), two intense peaks of the heat evolution were found on the calorimetric curves of the investigated samples. First, the active heat evolution is caused by wetting a cement powder and an initial kinetic reaction, during which Ca^{2+}, OH^{-}, SiO_4^{4-}, and SO_4^{2-} ions passed into the solution, and the second is related to the reaction between the deeper layers of calcium silicate particles and water [25]. In the second peak, at the later hydration period, a shoulder is also observed that is associated with an aluminate hydration reaction and with the final formation of ettringite [26].

The induction period of samples with the RWCD additive was found to be longer than in the OPC samples (50 min), and when 5, 15 or 20 wt% RWCD was used, this period endured for 1 h 12 min, 5 h 15 min, and 6 h 41 min, respectively (Fig. 5 (a)). During the hydration of cement samples with the RWCD additive, at the second exothermic reaction period, a later heat flow (compared to the pure cement sample) was identified on the released heat flow measurement curve (Fig. 5 (a)). It should be noted that the acceleration period in samples with the RWCD additive (except sample with 20 wt% RWCD) proceeds more intensively in comparison to plain Portland cement samples, as the height of the second peak of the heat evolution increases. Moreover, it was found that all samples with the RWCD additive up to 3 h of hydration (in sample with 5 wt% of the RWCD additive – the entire investigation period) emit more heat energy than the OPC sample (Fig. 5 (b)). Based on the obtained results, the RWCD additive increases the initial hydration of cement, yet prolongs the dormant period. The increased heat of the hydration may be attributed to the increased number of nucleation sites by RWCD for deposition of cement hydrates. This effect enhances the hydration after the dormant period [27]. Nevertheless, the substantial amount of chlorides in the chemical composition of RWCD also impacts on the acceleration of early cement hydration [28].

The investigation of the compressive strength of the samples with the RWCD additive showed that this additive had a positive

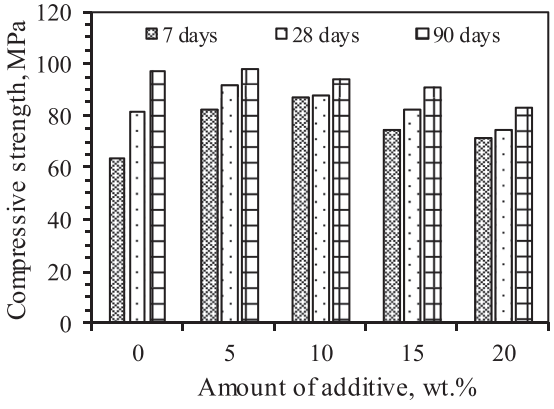

Fig. 6. Compressive strength of cement samples with different amounts of RWCD additive after 7, 28 and 90 days of hydration.

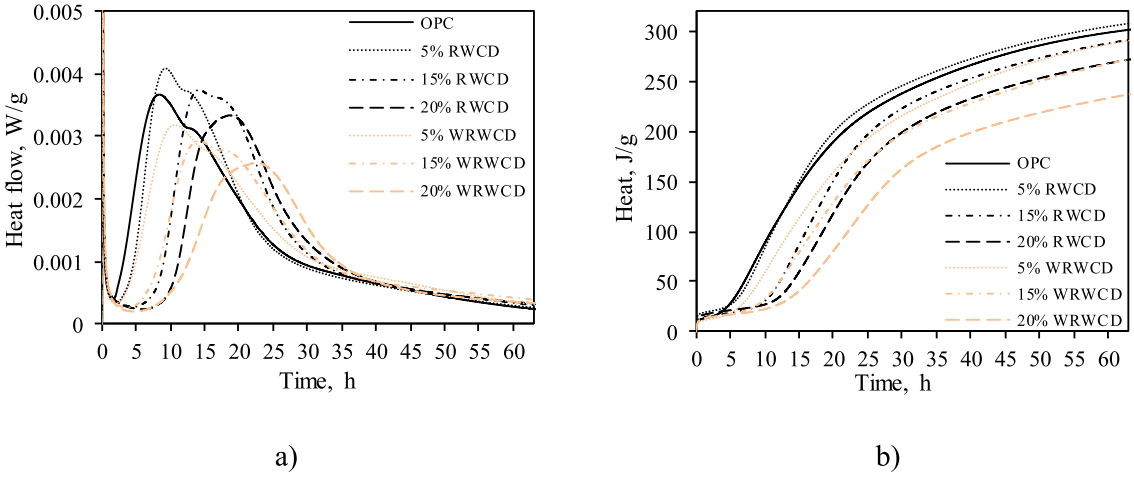

Fig. 5. Calorimetric curves of heat flow (a) and total heat (b) in samples with different amounts of the investigated additives.

effect on the compressive strength of samples up to 28 days of hydration (Fig. 6). After 7 days of hydration the compressive strength of all samples with the RWCD additive is higher than the compressive strength of pure OPC samples. After 28 days of hydration samples with 5 wt% RWCD additive had higher compressive strength (91.4 MPa), whereas samples with 15 wt% RWCD additive had the same compressive strength (82.1 MPa) as the OPC samples.

In contrast, after 90 days of hydration (Fig. 6), the compressive strength of all samples with the RWCD additive is lower than the compressive strength of plain OPC samples. The obtained data suggest that, with increasing duration of hardening, the compressive strength of samples with the additive increases noticeably slowly in comparison to the compressive strength of pure cement samples.

To clarify this phenomenon, the XRD analysis of hardened samples was performed.

The results of the XRD analysis (Fig. 7) showed that, after 28 and 90 days of hydration, in all X-ray patterns of the samples, the diffraction peaks of unhydrated tricalcium silicate (*d*-spacing: 0.304, 0.277, 0.260, 0.218 nm; JCPDS 42-0551) and unhydrated brownmillerite (*d*-spacing: 0.725 nm; JCPDS 30-0226) were identified. The diffraction peaks of quartz (*d*-spacing: 0.425, 0.334 nm; JCPDS 77-1060) were identified only in samples with the additive (Fig. 7 (a, b), curves 2–4) as SiO_2 is an integral part of this waste, and with an increasing amount of the additive, the intensity of the quartz peaks increases. Furthermore, in all XRD curves the characteristic peaks of calcite (*d*-spacing: 0.303, 0.228 nm; JCPDS 05-0586) were observed. In all samples with the RWCD additive (Fig. 7 (a, b), curves 2–4) among the ordinary hydration products (portlandite (*d*-spacing: 0.492, 0.311, 0.263, 0.193 nm; JCPDS 44-1481) and calcium silicate hydrates (*d*-spacing: 0.304, 0.279, 0.182 nm; JCPDS 33-0306)), Friedel's salt ($Ca_2Al(OH)_6Cl{\cdot}2H_2O$) (*d*-spacing: 0.789; 0.394; 0.288 nm; JCPDS 78-1219) was identified. The formation of this compound is associated with a considerable amount of Cl^- ions in the composition of the investigated waste. When increasing the amount of the additive and the duration of hardening, the intensity of Friedel's salt peaks also increases. Thus, this conversion of ordinary cement hydration products into non-cementitious materials (Friedel's salt) explains previously mentioned retarding of the compressive strength increasing in the samples with the RWCD additive. The results correspond to the investigation of other authors [29–31]. Besides, hydrated aluminasilicate (gismondine) was also identified in the samples with such additive.

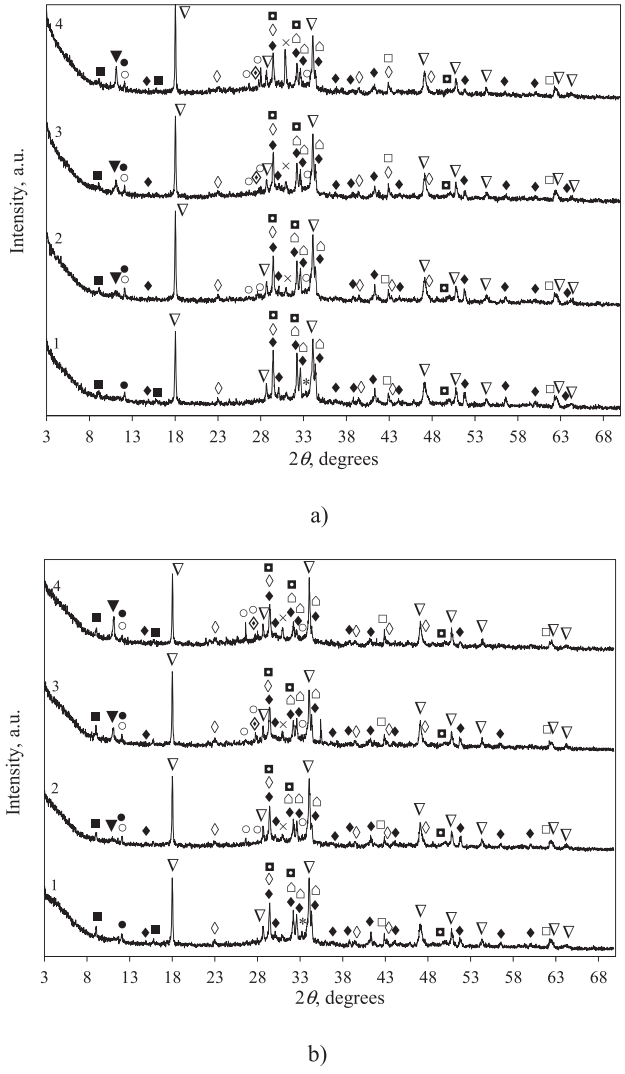

Fig. 7. X-ray diffraction patterns of cement samples with 0–20 wt% RWCD additive cured for 28 (a) and 90 (b) days under normal conditions: 1–0 wt%, 2–5 wt%, 3–15 wt %, 4–20 wt%. Indexes: ◊ – calcite ($CaCO_3$), ◆ – tricalcium silicate (Ca_3SiO_5), ○ – dicalcium silicate (Ca_2SiO_4); ● – brownmillerite ($4CaO{\cdot}Al_2O_3{\cdot}Fe_2O_3$); * – tricalcium aluminate ($Ca_3Al_2O_3$); ∇ – portlandite ($Ca(OH)_2$); ◘ – calcium silicate hydrate ($Ca_{1,5}SiO_{3,5}{\cdot}xH_2O$); ○ – gismondine ($CaAl_2Si_2O_8{\cdot}4H_2O$); ▼ – Friedel's salt ($Ca_2Al(OH)_6Cl(H_2O)_2$); ■ – ettringite ($Ca_6Al_2(SO_4)_3(OH)_{12}{\cdot}26H_2O$), × – dolomite ($CaMg(CO_3)_2$); ◊ – albite ($NaAlSiO_3O_8$); □ – periclase (MgO).

In all of the DSC curves (Fig. 8) of the hydrated samples, endothermic effects at 100–200 °C, 450–460 °C and ~700 °C were observed. The first endothermic peak belongs to the dehydration of many cement hydration products (such as calcium silicate hydrates, calcium aluminium hydrates, and ettringite), the endothermic effect at 435–465 °C indicates the decomposition of portlandite, whereas the endothermic effect at ~ 700 °C indicates the decomposition of calcite. Additionally, in the DSC curves of samples with 20 wt% RWCD additive (Fig. 8(a and b), curve 4), the endothermic peak at ~ 600 °C was observed. This endothermic effect indicates the presence of dolomite. Furthermore, in the DSC curves of samples with 15 and 20 wt% RWCD additive (Fig. 8 (a, b), curves 3, 4), the endothermic shoulder at ~320 °C was observed. This thermal effect belongs to the stepped decomposition of Friedel's salt. Friedel's salt is characterised by three thermal effects: endothermic effects at ~130 °C and ~320 °C and exothermal effect at ~640 °C [32,33]. In this case, the first endothermic effect coincides with the dehydration of many other ordinary cement hydration products, whereas the exothermal effect is overlapped by thermal effects of decomposition of carbonates.

The results of the TG analysis are listed in Table 3. The intensity of endothermic peaks and mass loss related with portlandite decomposition (~455 °C) decreased with growing content of the RWCD additive from 5 to 20 wt% in cement samples after 28 and 90 days of hydration (Fig. 8a and b; Table 3).

The distinctive character of the mass loss was visible in the area of other cement hydration products decomposition. After 28 days of hydration, the mass loss at 90–200 °C in all samples is closely similar; while after 90 days of hydration, the above-mentioned mass loss in all samples with the RWCD additive was higher than that in the pure samples. The highest mass loss was observed in the sample with 20 wt% of the RWCD additive.

Relatively high mass loss at 90–200 °C in samples with the RWCD additive after 28 and 90 days of hydration could be associated with the fact that the RWCD additive promoted the cement hydration reaction, yet the mass loss related with portlandite decomposition (~455 °C) decreased (Table 3). This phenomenon can be explained by Friedel's salt formation reaction. Friedel's salt

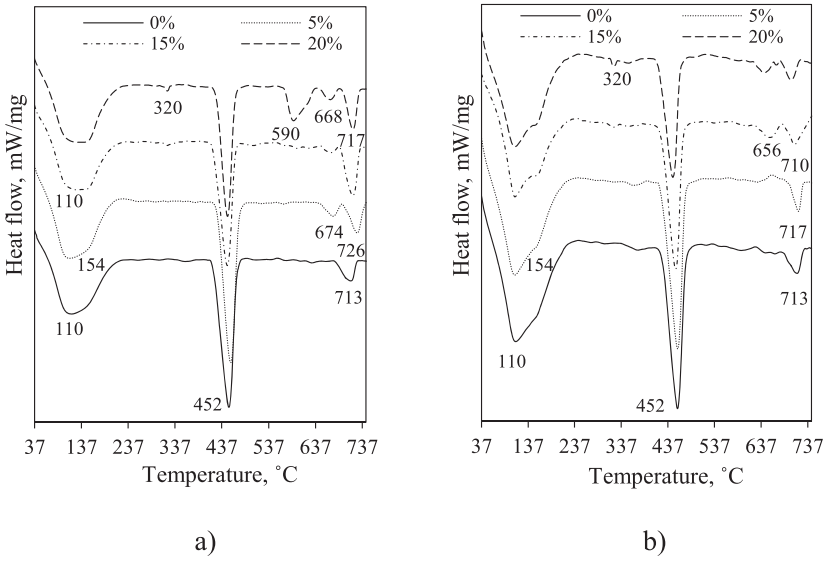

Fig. 8. Differential scanning calorimetry patterns of samples with different amount of the RWCD additive cured for 28 (a) and 90 (b) days under normal conditions.

Table 3
Thermogravimetric analysis results of samples cured for 28 and 90 days under normal conditions.

Amount of RWCD additive, wt.%	Mass loss, wt.%			
	After 28 days of hydration		After 90 days of hydration	
	90–200 °C	430–465 °C	90–200 °C	430–465 °C
0	4.77	2.34	5.16	2.86
5	4.80	2.34	5.25	2.37
15	4.80	2.24	5.34	2.12
20	4.84	1.70	5.44	1.60

was formed because of the reaction between calcium aluminate hydrates and chlorides through the following mechanism that implies two steps:

$$Ca(OH)_2 + 2NaCl\ (KCl) \rightarrow 2Na(K)(OH)_2 + CaCl_2$$

$$CaCl_2 + Ca_3Al_2O_6 \cdot 8H_2O + 2H_2O \rightarrow Ca_4Al_2O_6Cl_2 \cdot 10H_2O$$

The formation of Friedel's salt consumes some of the portlandite reserve [22,25,26], therefore the amount of portlandite has decreased with the increasing content of the RWCD additive in cement samples. On the other hand, the increase of mass loss at 90–200 °C in all samples with the RWCD additive can be related not only to the decomposition of ordinary cement hydrates, but also to the decomposition of Friedel's salt.

In terms of the results of the investigation, it can be assumed that the RWCD additive promotes the Friedel's salt formation throughout all hydration time and decreases the compressive strength of samples cured for 90 days. To avoid a negative effect on cement stone structure, the ground mineral cupola dust washed by water was carried out in the next stage of the research.

3.3. Influence of washed and ground mineral wool cupola dust waste on Portland cement hydration and hardening

RWCD was washed by water under laboratory conditions (water-to-solid material ratio (w/s) was 10, stirring time was 1, 5 and 10 min). It was found (Table 4) that washing had a positive effect on the reduction of chlorides. With increasing time of stirring from 1 to 10 min, the amount of Cl^- ions in the composition of dust decreased up to 0.689–0.612 wt% respectively. Since the stirring for longer than 5 min did not have a significantly affect in chlorides leaching, the dust waste after 5 min stirring (WRWCD) was used in the future research.

Table 4
Amount of Cl^- ions in the waste after washing at different time.

Sample	Stirring time, min	Amount of Cl^- ions in material, wt.%
RWCD	–	4.901
WRWCD	1	0.689
w/s = 10	5	0.612
	10	0.612

The same diffraction peaks typical to albite, dolomite, quartz, periclase and iron sulfite were identified in XRD patterns after RWCD washing (Fig. 9, curves 1-3) as well in raw cupola dust (Fig. 3). The main difference between the unwashed and washed waste XRD analysis data is related with sylvite and halite diffraction peaks. Peaks typical to halite disappeared, while only the low-intensity main peak of sylvite (*d*-spacing: 0.314 nm) was observed when suspension was stirred 1–10 min (Fig. 9, curves 1-3).

It should be noted, that the results of chemical analysis of WRWCD sample (Table 1) were in a good agreement with the data of XRD. After additional washing, the amount of K_2O, Na_2O and Cl was significantly reduced, while the quantity of SO_3 – remained almost the same. This data showed, that other compounds of cupola dust, except chlorides, are insoluble and their effect on hydration of investigated samples should be the same as in the case of RWCD additive. Furthermore, the washing of waste had no effect on

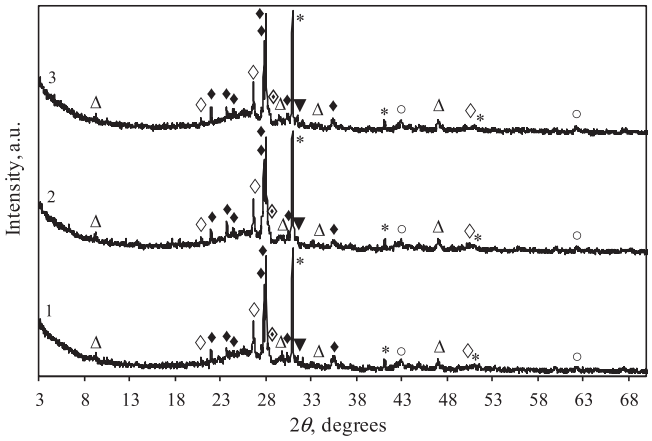

Fig. 9. X-ray diffraction pattern of washed dust waste, when w/s = 10 and stirring time: 1–1 min, 2–5 min, 3–10 min. Indexes: * – dolomite ($CaMg(CO_3)_2$); ◊ – quartz (SiO_2); ◆ – albite ($NaAlSiO_3O_8$); ▼ – iron sulfite ($FeSO_3$); Δ – paragonite ($NaAl_2(Si_3Al)O_{10}(OH)_2$); ○ – periclase (MgO); ⋄ – sylvite (KCl).

the pozzolanic activity of the investigated dust – cement samples with the WRWCD additive also do not satisfy the test for pozzolanicity (Fig. 4).

Calorimetric analysis data showed that the WRWCD additive prolonged the induction period of cement hydration as well as RWCD (Fig. 5, a). It was fixed that this period lasts about 1 h 17 min, 4 h 34 min and 6 h 27 min when 5, 15, and 20 wt% of WRWCD were used respectively, while induction period duration of the cement sample without admixture was 50 min. Furthermore, the heat flow released throughout all hydration time of all cement samples with WRWCD were lower than in samples with unwashed admixture or in the pure cement sample. These findings show that the increased heat of hydration of RWCD samples (Fig. 5, b) is attributed namely to the substantial amount of chlorides in the chemical composition of RWCD.

During the hydration of cement samples with the WRWCD additive, a later heat flow was identified on the released heat flow measurement curve at the second reaction period, compared to the pure cement sample (Fig. 5, a). The second peak of the released heat flow in the pure cement sample was fixed at 7 h 55 min, while in samples with 5 and 15 wt% WRWCD after 10 h 07 min and 14 h 24 min respectively. When 20 wt% of WRWCD additive was used, a C_3S hydration process is characterised by a negligible shoulder fixed at 19 h 29 min. The acceleration period in samples with the WRWCD additive (in contrast to the case with the RWCD additive) proceeds significantly slower compared to the plain Portland cement samples because the height of the second peak of the heat evolution decreases. Moreover, all samples with the WRWCD additive up to 60 h of hydration emitted less heat energy than the OPC sample (Fig. 5, b) and the emitted heat value was higher when the lower part of cement was replaced with this additive. Summarising the calorimetric research data, the results show that the WRWCD additive (in contrast to the case with the RWCD additive) retard the initial hydration of cement.

Even though both investigated additives (RWCD and WRWCD) had a different influence on the initial hydration process of Portland cement, the investigation of the compressive strength of the samples with the WRWCD additive showed that this admixture also had a positive effect on the compressive strength of samples (Fig. 10). After 7 days of hydration cement samples with 5–20 wt%

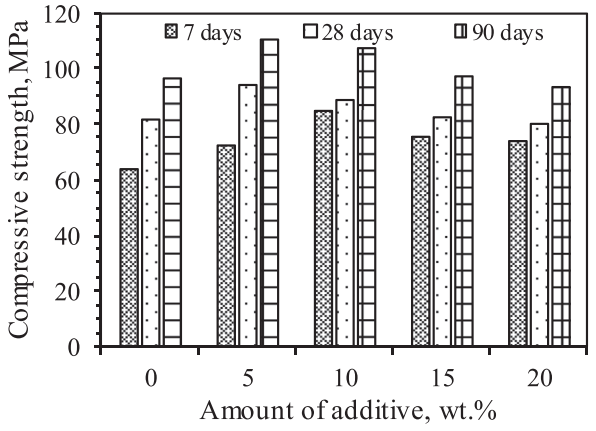

Fig. 10. Compressive strength of cement samples with different amounts of WRWCD additives after 7, 28 and 90 days of hydration.

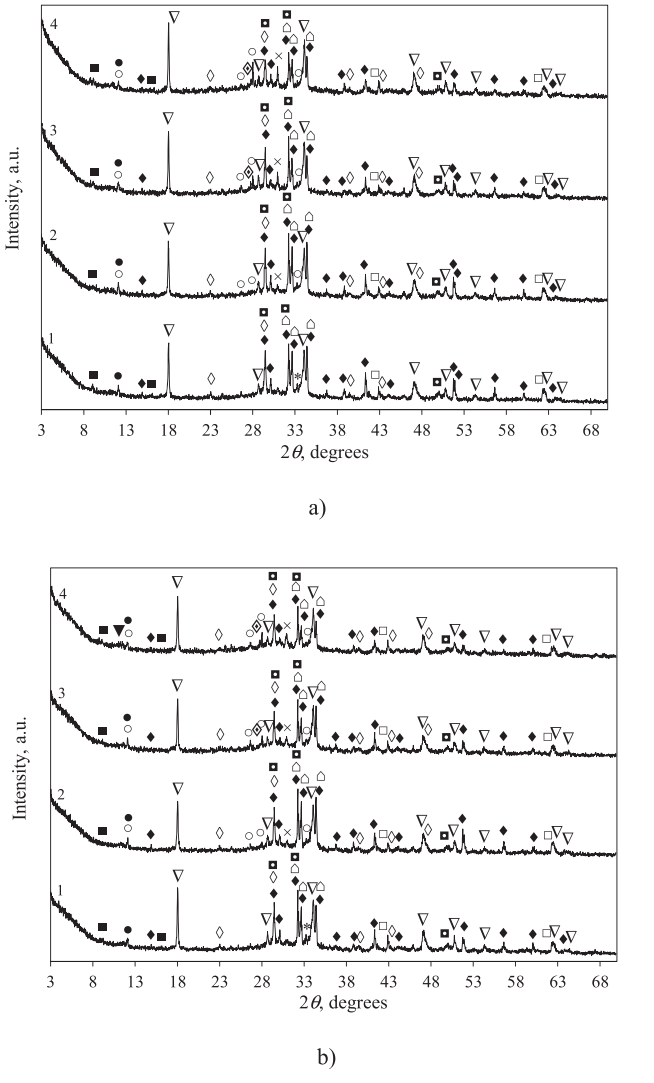

Fig. 11. X-ray diffraction patterns of cement samples with 0–20 wt% WRWCD additive cured for 28 (a) and 90 (b) days under normal conditions. 1–0 wt%, 2–5 wt%, 3–15 wt%, 4–20 wt%. Indexes: ◊ – calcite ($CaCO_3$), ◆ – tricalcium silicate (Ca_3SiO_5), ⌂ – dicalcium silicate (Ca_2SiO_4); ● – brownmillerite ($4CaO{\cdot}Al_2O_3{\cdot}Fe_2O_3$); * – tricalcium aluminate ($Ca_3Al_2O_3$); ∇ – portlandite ($Ca(OH)_2$); ◘ – calcium silicate hydrate ($Ca_{1,5}SiO_{3,5}{\cdot}xH_2O$); ○ – gismondine ($CaAl_2Si_2O_8{\cdot}4H_2O$); ▼ – Friedel's salt ($Ca_2Al(OH)_6Cl(H_2O)_2$); ■ – ettringite ($Ca_6Al_2(SO_4)_3(OH)_{12}{\cdot}26H_2O$), × – dolomite ($CaMg(CO_3)_2$); ⋄ – albite ($NaAlSiO_3O_8$); □ – periclase (MgO).

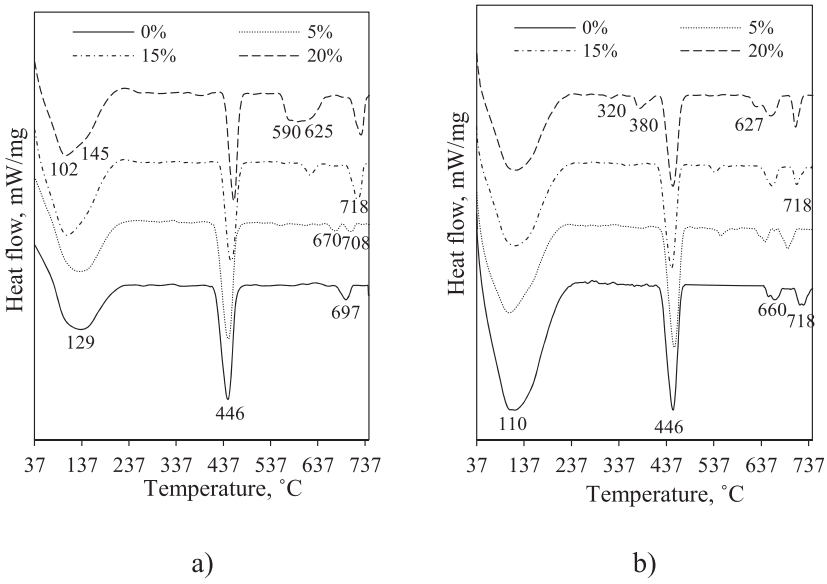

Fig. 12. Differential scanning calorimetry patterns of samples with different amount of the WRWCD additive cured for 28 (a) and 90 (b) days under normal conditions.

Table 5
Thermogravimetric analysis results of hydrated cement samples with 0–20 wt% of the WRWCD additive.

Amount of WRWCD additive, wt.%	Mass loss, wt.%			
	After 28 days of hydration		After 90 days of hydration	
	90–200 °C	430–465 °C	90–200 °C	430–465 °C
0	4.77	2.34	5.16	2.86
5	4.79	2.56	5.53	3.05
15	5.28	2.31	5.46	2.84
20	4.82	2.11	5.00	2.02

WRWCD had a higher compressive strength than OPC (64 MPa). The highest compressive strength (85 MPa) exhibited the sample with 10 wt% additive. It was determined that 28 days cured samples with 5, 10 and 15 wt% WRWCD additive (94, 89 and 82 MPa, respectively) had a higher compressive strength than OPC (81 MPa). Even when 20 wt% of WRWCD was used, the sample exhibited 80 MPa compressive strength. It was found that, when curing time was increased up to 90 days, samples with 5 and 10 wt% WRWCD additive had the highest compressive strength, 110 and 107 MPa, respectively; whereas the sample with 15 wt% additive had the same compressive strength as Portland cement samples without additive – 97 MPa.

Considering the research data, it can be stated that 5–15 wt% of WRWCD additive (in contrast to the RWCD additive) had a positive effect on the compressive strength of Portland cement samples throughout all investigated period. Thus, additional washing of waste dust is suitable in order to use this waste as an additive for Portland cement.

The results of the XRD analysis (Fig. 11) showed that the part of the tricalcium silicate, dicalcium silicate and brownmillerite remains unhydrated and the main hydration products such as portlandite, calcium silicate hydrate and ettringite in Portland cement samples with 0–20 wt% WRWCD additive form after 28 days of hydration. The intensity of diffraction peaks characteristic for calcium silicate hydrate (*d*-spacing: 0.304, 0.279, 0.182 nm; JCPDS 33-0306) and portlandite (*d*-spacing: 0.492, 0.311, 0.263, 0.192 nm; JCPDS 44-1481) grows with an increasing amount of the WRWCD additive from 5 to 20 wt%. Besides, the formation of gismondine (*d*-spacing: 0.730, 0.333, 0.318, 0.269 nm; JCPDS 39-1373) was observed in XRD curves (Fig. 11, a, curves 2–4) of Portland cement samples with the WRWCD additive.

The main difference between XRD curves of the Portland cement samples with washed and unwashed waste additive after 28 and 90 days of hydration is the identification of Friedel's salt. After 28 days of hydration the peaks characteristic of Friedel's salt was not identified in any samples, while only the obscure peak of this compound was found on the XRD curve of sample with 20 wt% of the WRWCD additive after 90 days of hydration (Fig. 11, b, curve 4). Thus, the reducing of chlorides amount in an investigated waste leads to the formation of a stable structure of the cement stone.

In all DSC curves (Fig. 12a and b) of the hydrated samples with the WRWCD additive the same, as in case with the RWCD additive, endothermic effects at 90–200 °C, 430–465 °C and 600–720 °C were observed. Additionally, the new endothermic effect at 380 °C, characteristic to brucite ($Mg(OH)_2$) decomposition [34,35], and negligible deflection at 320 °C (trace of Friedel's salt) was found in the DSC curve of the sample with 20 wt% WRWCD additive (Fig. 12, b, curve 4) after 90 days of hydration.

The results of the thermogravimetric analysis (Table 5) showed that, after 28 days of hydration, the highest mass loss related to portlandite decomposition was in the sample with 5 wt% of the WRWCD additive, while these mass losses in samples with 15 wt% of the WRWCD additive and pure OPC samples were approximately the same. With increasing duration of hydration time from 28 to 90 days, this trend persists. In the sample with 20 wt% of the WRWCD additive, a decrease of mass loss, related to portlandite

decomposition from 2.11 to 2.02 wt%, is fixed when the hydration time prolongs from 28 to 90 days. This reduction of mass loss is associated with already described Friedel's salt formation reaction, although only traces of Friedel's salt were identified from the data of the XRD and DSC analysis.

A higher mass loss of other cement hydration products (mainly calcium silicate hydrates) decomposition at 90–200 °C was fixed in all samples with the WRWCD additive than in the pure OPC sample after 28 days of hydration. When hydration time increases to 90 days, the mass loss at 90–200 °C remains highest in the samples with 5 and 15 wt% of the WRWCD additive, while this mass loss in the sample with 20 wt% additive already was lower than that of the OPC sample.

Thus, the WRWCD additive promotes the hydration process of Portland cement as both major cement clinker hydrates (calcium silicate hydrates and portlandite) are formed in the samples with this additive.

In conclusion, it can be stated, that RWCD additive increases the initial hydration of cement, however promotes the formation of Friedel's salt under all experimental conditions and decreases the compressive strength of samples. In contrary, WRWCD additive retard the initial hydration of cement, but promotes the hydration process of Portland cement at later period of hydration. Besides, it increases the compressive strength of samples. The reduction of chlorides amount in mentioned by-product leads to the formation of a stable structure cement stone, meanwhile the maximum admissible amount of washed and ground cupola dust waste is 15 wt %.

4. Conclusions

1. The main impurities of dust, collected in air filters during the melting of mineral wool raw materials are halite and sylvite. These impurities increase the initial hydration of cement and promote the formation of a significant amount of Friedel's salt in Portland cement mixtures with RWCD additive, and also decrease the compressive strength of samples, which were cured for 90 days.
2. The content of chlorides in the raw material was reduced from 4.901 to 0.612 wt% by washing with water when the water-to-solid ratio was equal to 10. Washed and ground cupola dust retards the initial hydration of cement, but has a positive effect on the compressive strength of the Portland cement samples. When 5, 10, and 15 wt% of prepared dust additive were used, the compressive strength of the samples after 28 and 90 days of hydration was greater than that of the pure Portland cement sample.
3. The reduction of chlorides amount in an investigated waste eliminates the crystallization of Friedel's salt and leads to the formation of a stable structure cement stone. Besides, it accelerates the hydration of calcium silicates and also promotes the formation of gismondine.

References

[1] K.B. Najim, Z.S. Mahmod, A.M. Atea, Experimental investigation on using cement kiln dust (CKD) as a cement replacement material in producing modified cement mortar, Construct. Build. Mater. 55 (2014) 5–12.
[2] N.A. Madlool, R. Saidur, M.S. Hossain, N.A. Rahim, A critical review on energy use and savings in the cement industries, Ren. Sus. En. Rev. 15 (4) (2011) 2042–2060.
[3] K. Sobolev, M. Arikan, High volume mineral additive ECO cement, Am. Ceram. Soc. Bull. 81 (1) (2002) 39–43.
[4] A. Korpa, T. Kowald, R. Trettin, Hydration behaviour, structure and morphology of hydration phases in advanced cement-based systems containing micro and nanoscale pozzolanic additives, Cement Concr. Res. 38 (7) (2008) 955–962.
[5] C. Jaturapitakkul, J. Tangpagasit, S. Songmue, K. Kiattikomol, Filler effect and pozzolanic reaction of ground palm oil fuel ash, Construct. Build. Mater. 25 (11) (2011) 4287–4293.
[6] M.S. Morsy, S.S. Shebl, Effect of silica fume and metakaoline pozzolana on the performance of blended cement pastes against fire, Ceram.-Silik 51 (1) (2007) 40–44.
[7] A. Shvarzman, K. Kovler, I. Schamban, G.S. Grader, G.E. Shter, Influence of chemical and phase composition of mineral admixtures on their pozzolanic activity, Adv. Cement Res. 14 (1) (2002) 35–41.
[8] R. Kaminskas, R. Kubiliute, Artificial pozzolana from silica gel waste–clay–limestone composite, Adv. Cement Res. 26 (3) (2014) 155–168.
[9] A.M. Dunster, Waste Mineral Fibre in Ceiling Tile Manufacture. Characterisation of Mineral Wastes, Resources and Processing Technologies – Integrated Waste Management for the Production of Construction Material, 2007, pp. 1–7 see also, http://www.smartwaste.co.uk/filelibrary/Ceiling_tiles_waste_mineral_wool.pdf. (Accessed 8 May 2017).
[10] A. Cheng, W.T. Lin, R. Huang, Application of rock wool waste in cement-based composites, Mater. Des. 32 (2) (2011) 636–642.
[11] A. Korpa, T. Kowald, R. Trettin, Hydration behavior, structure and morphology of hydration phases in advanced cement-based systems containing micro and nanoscale pozzolanic additives, Cement Concr. Res. 38 (7) (2008) 955–962.
[12] A. Askarinejad, A.R. Pourkhorshidi, T. Parhizkar, Evaluation the pozzolanic reactivity of sonochemically fabricated nano natural pozzolan, Ultrason. Sonochem. 19 (1) (2012) 119–124.
[13] L. Wei-Ting, C. An, H. Ran, Z. Si-Yu, Improved microstructure of cement-based composites through the addition of rock wool particles, Mater. Char. 84 (2013) 1–9.
[14] M. Michihiro, Resource recovery of inorganic solid waste for reduction of environmental load, J. Ceram. Soc. Jpn. 115 (1337) (2007) 1–8.
[15] T. Hattori, M. Matsuda, M. Miyake, Resource recovery of cupola dust: study on sorptive property and mechanism for hydrogen sulfide, J. Mater. Sci. 41 (12) (2006) 3701–3706.
[16] J. Žvironaitė, I. Pundienė, V. Antonovič, V. Balkevičius, Investigation of peculiarities in the hardening process of portland cements with active additives out of waste, Mater. Sci. Medzg 17 (1) (2011) 73–79.
[17] D. Korkmaz, Precipitation Titration: Determination of Chloride by the Mohr Method by dr. Deniz Korkmaz, see also, http://academic.brooklyn.cuny.edu/esl/gonsalves/tutorials/Writing_a_Lab_Report/xPrecipitation%20Titration%20edited%203.pdf. (Accessed 8 May 2017).
[18] M. Raverdy, F. Brivot, A.M. Paillére, R. Bron, Appreciation de l'activité pouzzolanique des constituents secondaires, in: Proc. 7th I.C.C.C. Paris, vol. 3, 1980, pp. 36–41.
[19] BSI British Standard, Methods of Testing Cement, Pozzolanicity Test for Pozzolanic Cement, 2005. BS EN 196–5.
[20] BSI British Standard, Methods of Testing Cement, Chemical Analysis of Cement, 2005. BS EN 196–2.
[21] BSI British Standard, Methods of testing cement, Methods of taking and preparing samples of cement, BS EN (2007) 196–197.
[22] BSI British Standard, Aggregates for concrete, BS EN 12620 (2008), 2002+A1.
[23] BSI British Standard, Methods of Testing Cement, Determination of Setting Times and Soundness, 2005. BS EN 196–3.
[24] BSI British Standard, Concrete. Specification, performance, production and conformity, EN 206 (2016), 2013+A1.
[25] D.G. Snelson, S. Wild, M. O'Farrell, Heat of hydration of Portland cement-metakaolin-fly ash (PC-MK-PFA) blends, Cement Concr. Res. 38 (6) (2008) 832–840.
[26] C. Hesse, F. Goetz-Neunhoeffer, J. Neubauer, A new approach in quantitative in-situ XRD of cement pastes: correlation of heat flow curves with early hydration reactions, Cem. Concr. Res. 41 (1) (2011) 123–128.
[27] B.W. Langan, K. Weng, M.A. Ward, Effect of silica fume and fly ash on heat of hydration of Portland cement, Cement Concr. Res. 32 (7) (2002) 1045–1051.
[28] X. Pang, P. Boul, W.C. Jimenez, Isothermal calorimetry study of the effect of chloride accelerators on the hydration kinetics of oil well cement, Construct. Build. Mater. 77 (2015) 260–269.
[29] I. Türkmen, Influence of different curing conditions on the physical and mechanical properties of concrete with admixtures of silica fume and blast furnace slag, Mater. Lett. 57 (29) (2003) 4560–4569.
[30] O.R. Ogirigbo, J. Ukpata, Effect of chlorides and curing duration on the hydration and strength development of plain and slag blended cements, J. Civ. Eng. Res. 7 (1) (2017) 9–16.
[31] U. Birnin-Yauri, F. Glasser, Friedel's salt, $Ca_2Al(OH)_6(Cl,OH)\cdot 2H_2O$: its solid solutions and their role in chloride binding, Cement Concr. Res. 28 (12) (1998) 1713–1723.
[32] J. Csizmadia, G. Balázs, F.D. Tamás, Chloride ion binding capacity of aluminoferrites, Cement Concr. Res. 31 (4) (2001) 577–588.
[33] J. Xu, C. Zhang, J. Linhua, L. Tang, G. Guofu, Y. Xu, Releases of bound chlorides from chloride-admixed plain and blended cement pastes subjected to sulfate attacks, Construct. Build. Mater. 45 (2013) 53–59.
[34] J. Wei, Q. Yu, W. Zhang, H. Zhang, Reaction products of MgO and microsilica cementitious materials at different temperatures, J. Wuhan Univ. Technol.-Materials Sci. Ed. 26 (4) (2011) 745–748.
[35] D. Stephan, S.N. Dikoundou, G. Raudaschl-Sieber, Hydration characteristics and hydration products of tricalcium silicate doped with a combination of MgO, Al_2O_3 and Fe_2O_3, Thermochim. Acta 472 (1–2) (2008) 64–73.